DOI: 10.1002/ejoc.200801012

Selective Positioning of CB[8] on Two Linked Viologens and Electrochemically Driven Movement of the Host Molecule

Samir Andersson,[a] Dapeng Zou,[a] Rong Zhang,[b] Shiguo Sun,[b] Björn Åkermark,[c] and Licheng Sun*[a]

Keywords: Cyclic voltammetry / Host-guest systems / Molecular devices / Inclusion compounds / Supramolecular chemistry

The binding interactions between cucurbit[8]uril (CB[8]) and a dicationic guest *N*,*N*-dimethyl-3,3′-dimethyl-4,4′-bipyridinium (DMV^{2+}) have been investigated by various experimental techniques including NMR, ESI-MS, and UV/Vis and fluorescence spectroscopy. In a three-component system consisting of CB[8], *N*,*N*-dimethyl-4,4′-bipyridinium (MV^{2+}) and DMV^{2+}, CB[8] was found to exhibit a higher binding affinity to DMV^{2+} than to MV^{2+}. When DMV^{2+} was connected to MV^{2+} by an alkyl chain, the first equiv. of CB[8] could be selectively positioned on the DMV^{2+} moiety, and then a second equiv. of CB[8] was positioned on the MV^{2+} moiety. Spectroelectrochemical studies showed that upon the reduction of this system at –0.6 V vs. AgCl, the CB[8] could move from the DMV^{2+} moiety to the $MV^{+\cdot}$ radical, which formed a dimer inside the CB[8] cavity. Molecular oxygen quenched the dimer, and the CB[8] moved back to the DMV^{2+} moiety, indicating a molecular movement driven by electrochemistry.

Introduction

In recent years, the macromolecular hosts of the cucurbit[*n*]uril (CB[*n*]) family have been extensively studied. In contrast to the cyclodextrins, CBs have cavities with polar edges and are especially suited for holding cationic species such as bipyridinium, ammonium, ferrocene and metal ions.[1–8] A common guest is methylviologen (*N*,*N*-dimethyl-4,4′-bipyridinium, MV^{2+}),[9–23] which is an efficient electron acceptor used for the construction of molecular devices.[13,24–27] Recently, several groups have reported the movement of a CB[*n*] host to different positions of a guest using either cyclodextrins or proton- and electron-transfer reactions.[20,28–33] It has previously been shown that dimethylmethylviologen (*N*,*N*-dimethyl-3,3′-dimethyl-4,4′-bipyridinium, DMV^{2+}, Figure 1) is more difficult to reduce than MV^{2+}. This property has been used to construct a light-driven molecular machine.[24,34] We have also presented a system with $Ru(bpy)_3$-MV^{2+} and CB[7] or CB[8], where a $Ru(bpy)_3$-$MV^{+\cdot}$ radical dimer locked inside one CB[8] was observed after photoinduced electron transfer.[26–27] Herein, we report the interactions between the host molecule CB[8] and guests $DMV^{2+}$and MV^{2+} and **1** and **2**, in which DMV^{2+} and MV^{2+} are connected by a 3- or 6-carbon chain, respectively (see Figure 1). ^1H NMR, ESI-MS, UV/Vis spectroscopy and spectroelectrochemistry were used to investigate these interactions. The movement of CB[8] along the carbon linker of the guest molecules, driven by one-

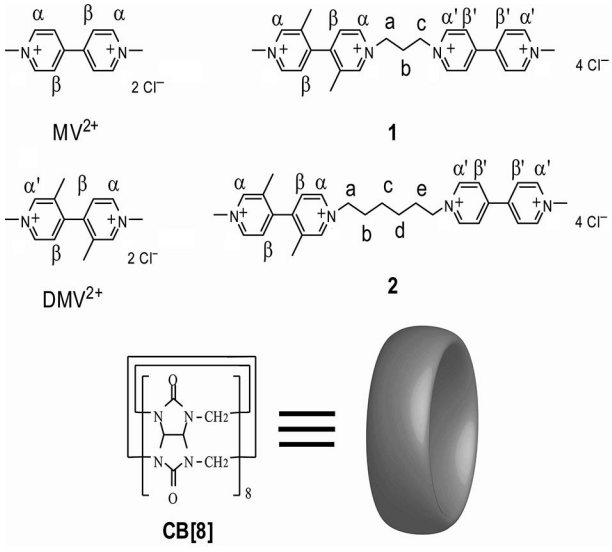

Figure 1. The chemical structures of MV^{2+}, DMV^{2+}, **1**, **2** and CB[8].

[a] School of Chemical Science and Engineering, Department of Chemistry, Royal Institute of Technology (KTH), Teknikringen 30, 10044 Stockholm, Sweden
Fax: +46-8-7912333
E-mail: lichengs@kth.se
[b] State Key Laboratory of Fine Chemicals, DUT-KTH Joint Education and Research Center on Molecular Devices, Dalian University of Technology (DUT), Zhong Shan Road 158-40, 116012 Dalian, China
[c] Department of Organic Chemistry, Arrhenius Laboratory, Stockholm University, 106 91 Stockholm, Sweden
Supporting information for this article is available on the WWW under http://www.eurjoc.org or from the author.

electron reduction at a controlled potential, was observed; molecular oxygen made the CB[8] move back to the original position.

Results and Discussion

Interaction of DMV^{2+} with CB[8]

We observed the formation of an inclusion complex between DMV^{2+} and CB[8] clearly by ^1H NMR (Figure 2). The β protons of the viologen residue exhibited an upfield shift from 7.97 to 6.74 ppm, while the α and α′ protons shifted upfield from 8.84 and 8.94 to 8.69 and 8.44 ppm, respectively, and the protons of methyl groups on the β position shifted upfield from 2.29 to 1.59 ppm. The *N*-methyl protons shifted slightly downfield, from 4.47 to 4.56 ppm, which meant that the α, β and β-methyl groups were all inside the cavity of CB[8], while the *N*-methyl groups were outside. This complexation-induced, ^1H NMR shift is consistent with those of the related systems reported by Kaifer et al.[10,35–36] and Kim et al.[11–12]

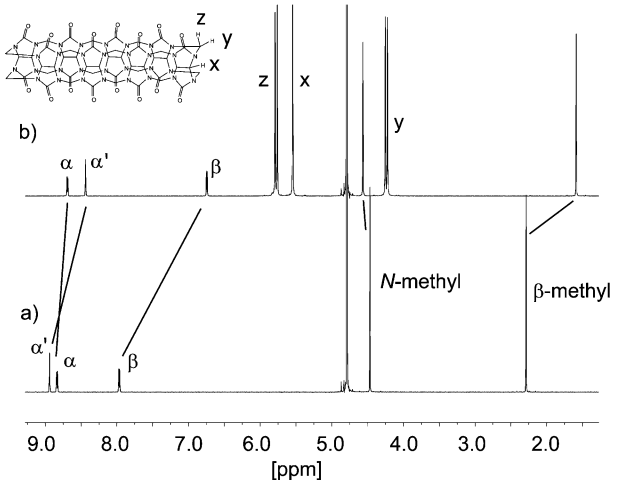

Figure 2. ^1H NMR spectra (500 MHz, D_2O) of DMV^{2+} in the (a) absence or (b) presence of CB[8] (1 equiv.).

We further demonstrated the formation of a 1:1 inclusion complex between DMV^{2+} and CB[8] by HRMS studies. When we dissolved equivalent amounts of DMV^{2+} and CB[8] in water, the HRMS gave a doubly charged peak at m/z = 771.2682 (calculated for $[DMV^{2+} + CB[8] - 2Cl^-]^{2+}$ 771.2698), which corresponds to the inclusion of DMV^{2+} into the cavity of CB[8] (see Figure 3). Thus, both ^1H NMR and HRMS results provided strong evidence for the formation of the 1:1, host-guest, inclusion complex between DMV^{2+} and CB[8].

Contrary to MV^{2+}, DMV^{2+} showed weak fluorescence with a maximum emission at approximately 363 nm, similar to the results previously reported for Diquat (DQ^{2+}, Scheme 1).[23] However, the emission of DMV^{2+} decreased

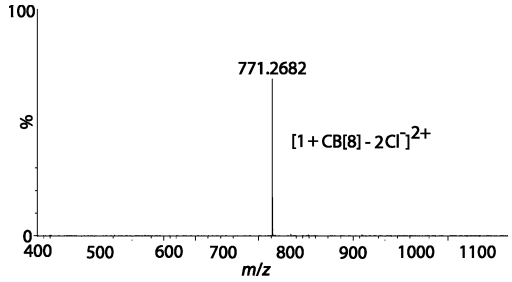

Figure 3. HRMS spectrum of the 1:1 inclusion complex of DMV^{2+} with CB[8].

significantly upon the addition of CB[8] (Figure 4, bottom panel). It is likely that the inclusion of DMV^{2+} into the cavity of CB[8] forces the pyridine rings into a less planar conformation, resulting in a quenching of the emission.[37] This assumption is also supported by the fact that the emission from rigid molecules such as DPT^{2+} (λ_{max} = 405 nm) and DAP^{2+} (λ_{max} = 449 nm),[35–36] increases upon inclusion into CB[8] (see Scheme 1).

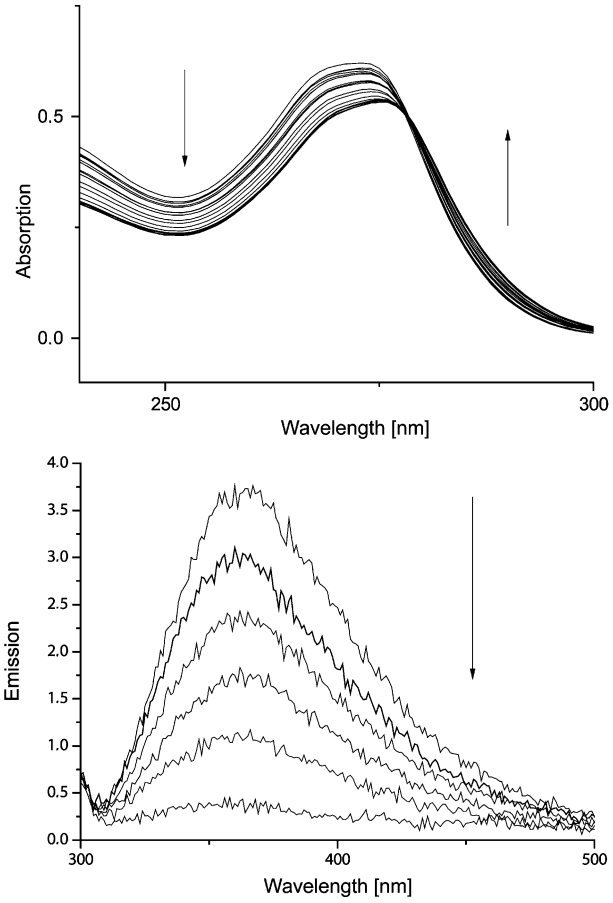

Figure 4. Absorption (top panel) and emission (bottom panel) spectrum of DMV^{2+} at a concentration of 5×10^5 L mol^{-1} alone or in the presence of increasing amounts (0–2 equiv. for the top panel and 0–1 equiv. for the bottom panel) of CB[8]; CB[8] increases concentration in the direction of the arrows.

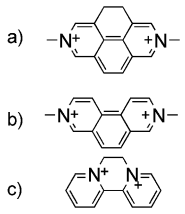

Scheme 1. The structures of (a) DAP^{2+}, (b) DPT^{2+} and (c) DQ^{2+}.

The absorption band at approximately 273 nm decreased when we added increasing amounts of CB[8] to the solution of DMV^{2+} in distilled water. We further verified the stoichiometry of the binding of DMV^{2+} with CB[8] by UV/Vis absorption titration measurements. We processed the data with OriginPro software and could easily fit the data to a 1:1 binding model. We calculated the binding constant to be $(2.6 \pm 0.3) \times 10^5$ L mol^{-1}, which is slightly greater than the value of 1.1×10^5 L mol^{-1} for MV^{2+} binding with CB[8], as reported earlier by Kim et al.[12]

Due to the difference in binding constants, we found an extraordinary preference for the binding of DMV^{2+} with CB[8] when a mixture of MV^{2+}, DMV^{2+} and CB[8] in equivalent amounts was dissolved in water (Scheme 2). The ^{1}H NMR peaks of DMV^{2+} showed upfield shifts, while the peaks for MV^{2+} were essentially unaffected (Figure 5, c). Although MV^{2+} did not give a measurable amount of inclusion complex formation, it did interfere with the binding of DMV^{2+} into the cavity of CB[8]. This was shown by the fact that the ^{1}H NMR peaks of DMV^{2+} broadened after the inclusion of DMV^{2+} into CB[8] in the presence of MV^{2+}, suggesting a dynamic interaction between DMV^{2+} and CB[8]. The dynamics of the system were also shown by the broadening of the MV^{2+} signals, which was slight at a DMV^{2+}/MV^{2+}/CB[8] ratio of 1:1:0.5 (Figure 5, b) but clearly visible at a 1:1:1 ratio (Figure 5, c). At a 1:1:2 ratio, finally, the MV^{2+} peaks also sharpened and shifted considerably (Figure 5, d). This confirmed that both DMV^{2+} and MV^{2+} were bound to CB[8].

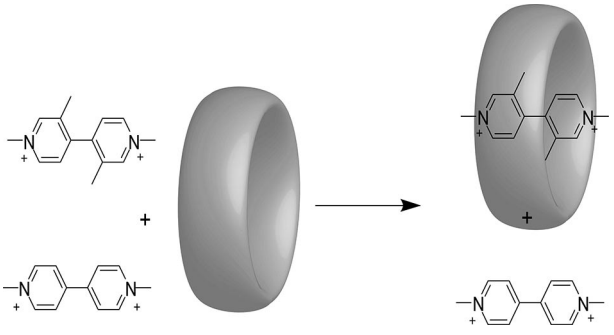

Scheme 2. The selective binding of CB[8] with DMV^{2+} in a mixture of DMV^{2+}, MV^{2+} and CB[8] (1:1:1) in water.

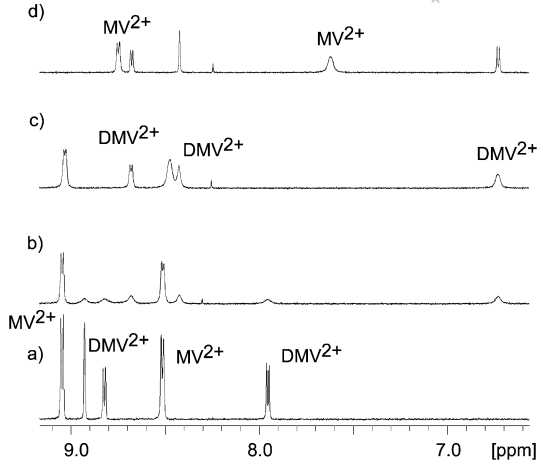

Figure 5. ^{1}H NMR spectra (500 MHz, D_2O) of a DMV^{2+}/MV^{2+} mixture (both compounds at 3.8 mM) and CB[8] at different molar ratios: (a) 1:1:0, (b) 1:1:0.5, (c) 1:1:1 and (d) 1:1:2.

Electrochemistry of DMV^{2+}

For comparison, we studied the electrochemistry of both DMV^{2+} and MV^{2+} in acetonitrile and phosphate buffer at pH 7 (Table 1 and Figure 6).

In agreement with previous reports, both MV^{2+} and DMV^{2+} showed two reversible waves in acetonitrile, with MV^{2+} being the most easily reduced.[24,34] In aqueous solution, however, the redox potentials of both DMV^{2+} and MV^{2+} shifted to more negative values, as seen in the bottom panel of Figure 6. We observed the greatest change for DMV^{2+}, which showed only one reversible wave at –1.065 V vs. SCE. This value was even lower than that of the second reduction of MV^{2+} at –0.890 V vs. SCE. This meant that, in aqueous solution, MV^{2+} was doubly reduced before the first reduction of DMV^{2+} occurred.

To investigate how CB[8] influences the electrochemistry of DMV^{2+}, we performed CV measurements in the presence of 0.5 and 1 equiv. of CB[8], as shown in the top panel of Figure 7. As the amount of CB[8] increased from 0 to 1 equiv., the intensity of the reduction wave at –1.065 V vs. SCE decreased and shifted to –1.08 V (Figure 7), a negative shift of about 15 mV. A similar behaviour has been observed for MV^{2+} and CB[7], where inclusion induced a small negative shift of 20 mV.[10] A reasonable explanation is that the $DMV^{+\cdot}$ is, like $MV^{+\cdot}$ in CB[7], stabilised inside the CB[8] cavity. In contrast, Kim et al. found that $MV^{+\cdot}$ formed a dimer inside the cavity of CB[8], inducing a positive shift.[12]

In order to analyze further the interaction between DMV^{2+} and the host CB[8], we performed spectroelectrochemistry. After degassing the solution of DMV^{2+} with nitrogen, we introduced electrons at –1.1 V vs. Ag/AgCl. We observed the characteristic peaks of the radical cation $DMV^{+\cdot}$ at 390 and 790 nm[24,38–39] as well as a peak at 315 nm (Figure 7, bottom panel). The origin of this last peak is not clear, but it could derive from either the doubly reduced DMV^0 species or the $DMV^{+\cdot}$ radical pair. When

Table 1. The reduction potentials of DMV^{2+}, MV^{2+}, **1** and **2** in acetonitrile and water vs. SCE.

Entry	Compound	$E_{1/2}(1)$ [V][a]	$E_{1/2}(2)$ [V][b]	$E_{1/2}(3)$ [V][c]	$E_{1/2}(4)$ [V][d]
1	MV^{2+} in MeCN	–0.462	–0.879	–	–
2	DMV^{2+} in MeCN	–0.848	–1.037	–	–
3	**1** in MeCN	–0.413	–0.740	–0.906	–1.036
4	**2** in MeCN	–0.453	–0.854	–0.854	–1.032
5	MV^{2+} in H_2O	–0.643	–0.890	–	–
6	DMV^{2+} in H_2O	–1.065	–	–	–
7	**1** in H_2O	–0.564[e]	–0.805[e]	–0.987[e]	–
8	**2** in H_2O	–0.584[e]	–0.896[e]	–	–

[a] Half-wave potential for the first reduction process expressed in volts vs. SCE. The reference electrode was Ag/Ag^+ in MeCN and Ag/AgCl in pH 7 buffer and was measured at a scan rate of 0.05 $V s^{-1}$. The working electrode was a glassy carbon disk (3 mm diameter). [b] For the second reduction process. [c] For the third reduction process. [d] For the fourth reduction process. [e] Differential Pulse Voltammetry (DPV) values.

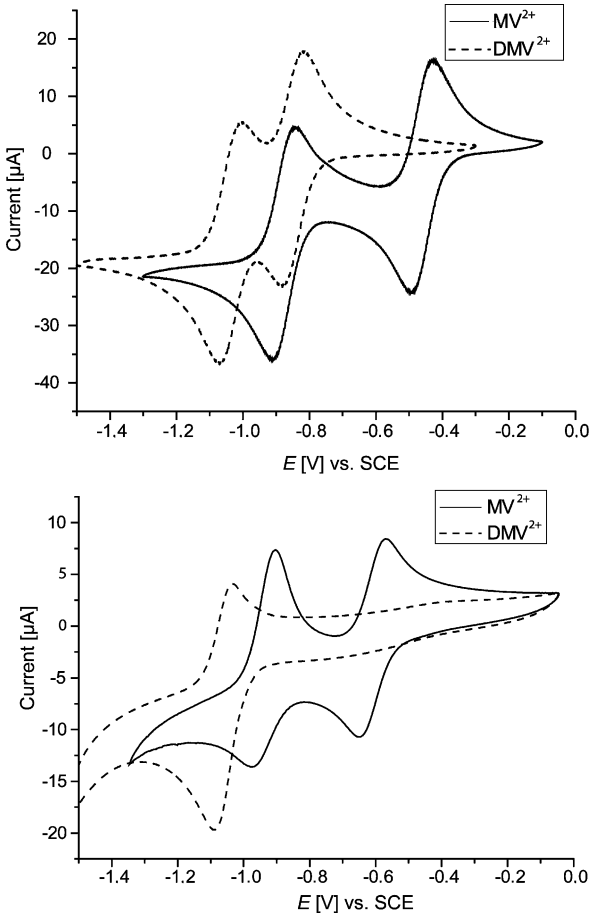

Figure 6. Cyclic voltammograms (CVs) of 1 mM DMV^{2+} (dashed) and MV^{2+} (solid) in MeCN (top panel) and in pH 7 phosphate buffer (bottom panel). The reference electrode was Ag/Ag^+ in MeCN and Ag/AgCl in pH 7 buffer and was measured at a scan rate of 0.05 $V s^{-1}$. The working electrode was a glassy carbon disk (3 mm diameter).

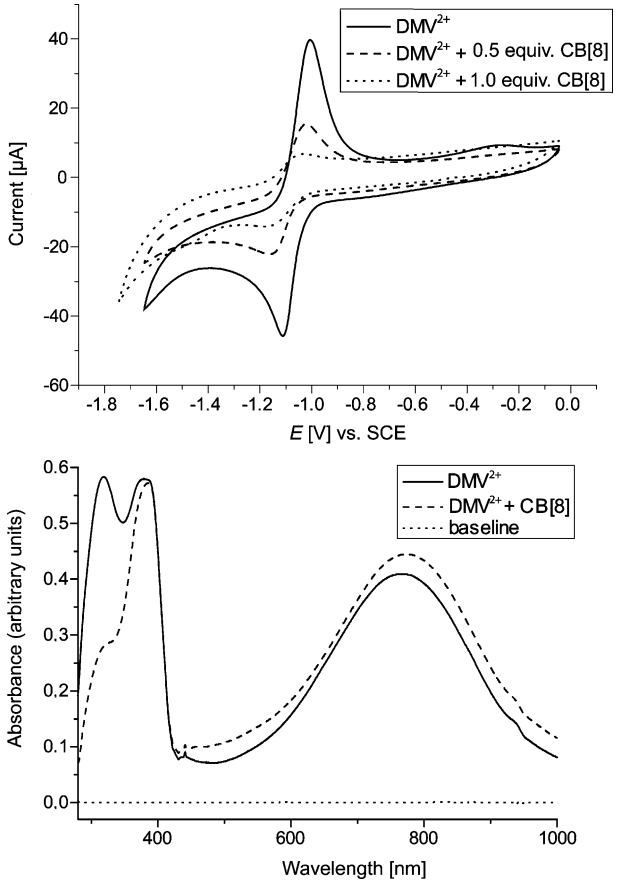

Figure 7. Cyclic voltammograms of DMV^{2+} (top panel) at 1 mM concentration with increasing amounts of CB[8] [solid (1:0), dashed (1:0.5) and dotted (1:1) lines]; the reference electrode (Ag/AgCl in pH 7 buffer) was measured at a scan rate of 0.05 $V s^{-1}$. The working electrode was a glassy carbon disk (3 mm diameter). UV/Vis spectroelectrochemistry (bottom panel) of DMV^{2+} at 5 mM (solid line), with 1 equiv. of CB[8] (dashed line) at –1.1 V vs. Ag/AgCl. The dotted line is the baseline.

we added 1 equiv. of CB[8] to the solution of DMV^{2+}, the intensity of the peak at 315 nm strongly decreased while the peaks at 390 and 790 nm were essentially unaffected. This indicated that the $DMV^{+\cdot}$ radical was stabilised inside the CB[8] cavity. We conducted the electrochemistry and spectroelectrochemistry at several concentrations of DMV^{2+} and amounts of CB[8] but found no changes in the electrochemistry or any new spectral peaks. Both the spectroelectrochemical and electrochemical measurements performed led to the conclusion that DMV^{2+} did not form a dimer inside the CB[8] cavity in its radical form. DMV^{2+} was instead stabilised only as a monomer inside CB[8]. A possible reason is the two $-CH_3$ groups in DMV^{2+}, which fill the

cavity of CB[8] and hinder the entrance of a second DMV^{2+} molecule. The same conclusion has been reached for DQ^{2+}.[23]

Interactions of 1 and 2 with CB[8]

From the work of Kim et al., it has been shown that the $MV^{+\cdot}$ dimer binds to CB[8] with a binding constant of 2×10^7 M^{-1}, about two orders of magnitude stronger than the binding of DMV^{2+}.[12–13,40] Since MV^{2+} is easier to reduce than DMV^{2+}, and the $DMV^{+\cdot}$ radical could not form a dimer inside the CB[8] (see the discussion above), it should be possible to design a system with both DMV^{2+} and MV^{2+} where CB[8] first binds to the DMV^{2+}, then upon the one-electron reduction of MV^{2+}, CB[8] exchanges DMV^{2+} for the $MV^{+\cdot}$ radical, which can form a dimer inside CB[8]. With this idea in mind, we synthesized **1** and **2** using a 3- or 6-carbon linker (Figure 1 and the Supporting Information).

The top panel of Figure 8 shows the ^{1}H NMR spectra of **1** in D_2O. The addition of 0.5 and 1.0 equiv. of CB[8] shifted the peaks corresponding to the DMV^{2+} moiety upfield. The two pairs of doublets from the β protons shifted upfield from 8.07 and 7.97 to 6.88 and 6.78 ppm, respectively. The signals from the α protons shifted upfield from 9.10 and 8.86 to 8.51 and 8.49 ppm and from 9.00 and 8.85 to 8.83 and 8.72 ppm, respectively, while the signals of the β-methyl groups shifted upfield from 2.33 and 2.31 to 1.67 and 1.65 ppm, respectively. These values are close to those of the proton shifts of DMV^{2+} upon its inclusion into the cavity of CB[8] (Figure 2). The a, b and c protons of the linker at 5.00, 2.93 and 4.94 ppm, respectively, as well as the α′ protons of the methylviologen at 9.24 ppm shifted downfield, indicating that they were located outside the CB[8] cavity. From the detailed ^{1}H NMR investigation, the position of CB[8] on **1** is proposed to be on the DMV^{2+} moiety. We observed similar phenomena for **2** as well (Figure 8, bottom panel). This configuration can also be seen by focusing on the CB[8] host, where the z protons split upon the addition of guest, indicating that the cavity sidewalls were in different environments (see the Supporting Information).

When we added 2 equiv. of CB[8] to **1**, we observed a weak interaction between the second CB[8] and the MV^{2+} moiety under NMR conditions, indicating a dynamic interaction. The ^{1}H NMR signals from the MV^{2+} moiety shifted upfield and was strongly broadened, showing that MV^{2+} was also inserted into a CB[8] cavity but in a dynamic fashion (Figure 8, d in the top panel). This is probably steric hindrance due to the short linkage (3-carbon chain) between the DMV^{2+} and MV^{2+} moieties. The behaviour of **2**, which has a longer linkage, was somewhat different. After the addition of 2 equiv. of CB[8] to **2**, all the ^{1}H NMR peaks sharpened and shifted considerably (Figure 8, d in the bottom panel). All the protons of the MV^{2+} moiety shifted upfield, while the protons of the linker shifted even more downfield, indicating the formation of a stable 1:2 inclusion complex between **2** and CB[8], as shown in Scheme 3 (see the Supporting Information).

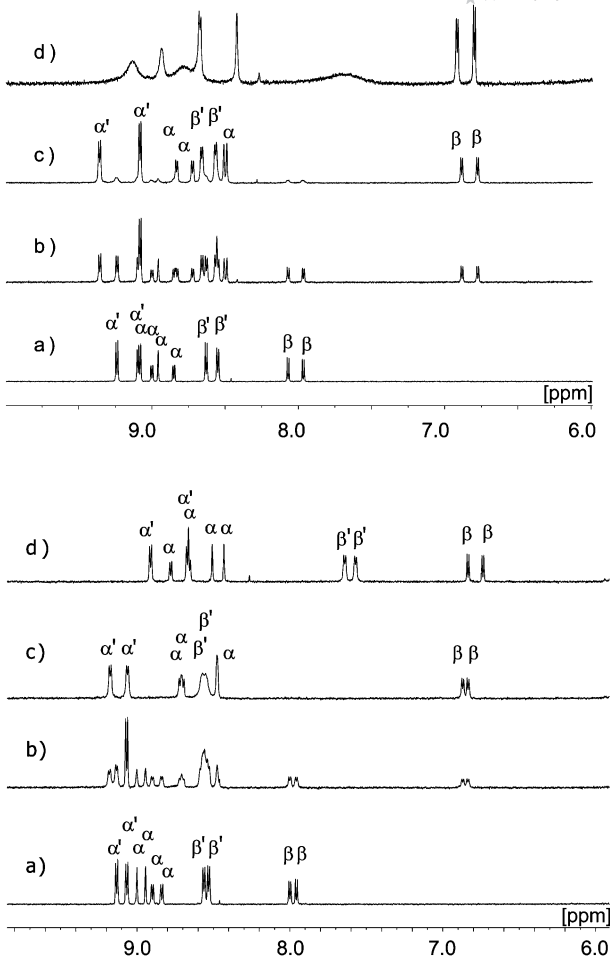

Figure 8. ^{1}H NMR (500 MHz, D_2O) of **1** (top, 3.8 mM) and **2** (bottom, 3.6 mM) in the absence (a) or presence of (b) 0.5, (c) 1.0 or (d) 2.0 equiv. of CB[8] at 25 °C in D_2O.

We further confirmed the formation of the inclusion complexes of **1** and **2** with CB[8] by HRMS. When we added 1 equiv. of CB[8] to a solution of **1** in water, the HRMS produced a quadruply charged peak at m/z = 435.1648 (calculated for $[\mathbf{1} + CB[8] - 4Cl^-]^{4+}$ 435.1638). When we added excess CB[8], the HRMS produced a quadruply charged peak at m/z = 767.5124 (calculated for $[\mathbf{1} + 2CB[8] - 4Cl^-]^{4+}$ 767.5126). Similarly, when we added 1 equiv. or an excess of CB[8] to a solution of **2** in water, the HRMS produced a quadruply charged peak at m/z = 445.6745 (calculated for $[\mathbf{2} + CB[8] - 4Cl^-]^{4+}$ 445.6755) or m/z = 777.7762 (calculated for $[\mathbf{2} + 2CB[8] - 4Cl^-]^{4+}$ 777.7737), respectively (see the Supporting Information).

Electrochemistry of 1 and 2

To investigate the high selectivity and the possible response of molecular movement of CB[8] upon reduction, we studied the electrochemistry of **1** and **2** both in acetonitrile and in a pH 7 phosphate buffer (Figures 9 and 10).

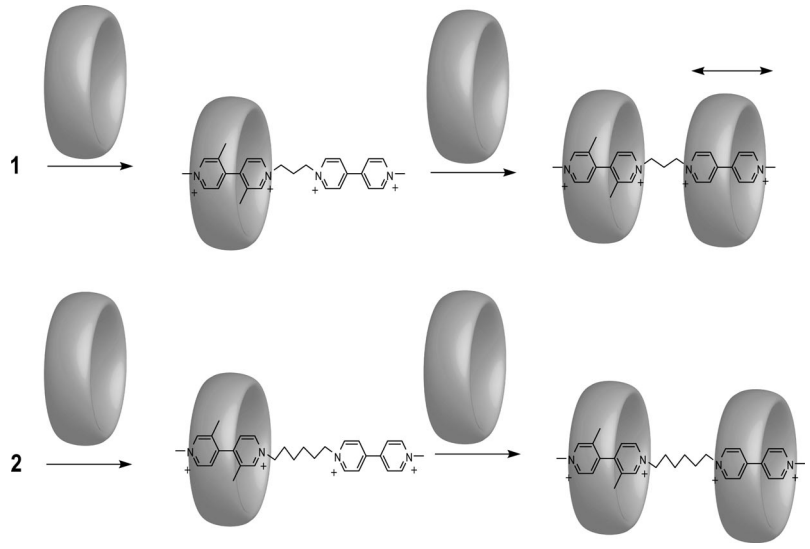

Scheme 3. Selective positioning of CB[8] on molecular dyads **1** and **2**.

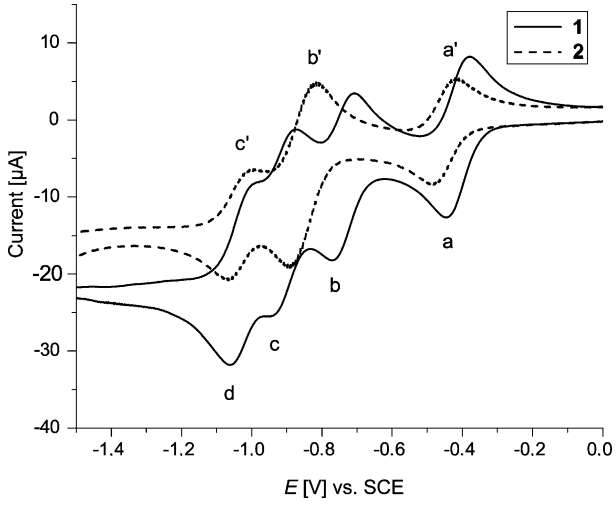

Figure 9. Cyclovoltammograms of **1** (solid line) and **2** (dashed line) at 0.5 mM in acetonitrile with a scan rate of 0.05 V s^{-1}. The reference electrode was Ag/Ag^+ in MeCN. The working electrode was a glassy carbon disk (3 mm diameter). The reversible reduction peaks are assigned as: (a) $MV^{2+}/MV^{+\cdot}$, (b) $DMV^{2+}/DMV^{+\cdot}$, (c) $MV^{+\cdot}/MV^0$, (d) $DMV^{+\cdot}/DMV^0$, (a′) $MV^{2+}/MV^{+\cdot}$, (b′) $DMV^{2+}/DMV^{+\cdot}$ and $MV^{+\cdot}/MV^0$, (c′) $DMV^{+\cdot}/DMV^0$.

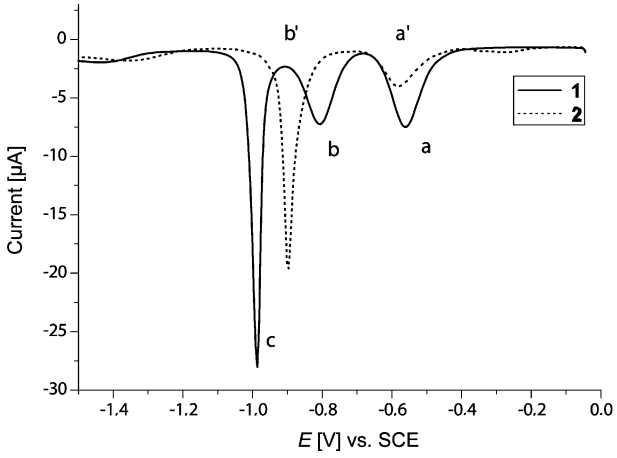

Figure 10. Differential pulse voltammograms of **1** (solid line) and **2** (dashed line) at 0.5 mM in a pH 7 phosphate buffer. The working electrode was a glassy carbon disk (3 mm diameter). The reduction peaks are assigned as: (a) $MV^{2+}/MV^{+\cdot}$, (b) $DMV^{2+}/DMV^{+\cdot}$ for **1** and (a′) $MV^{2+}/MV^{+\cdot}$ for **2**.

In acetonitrile, the CV of **1** showed four reversible waves (solid line in Figure 9), which were assigned to the reductions $MV^{2+} \rightarrow MV^{+\cdot}$, $DMV^{2+} \rightarrow DMV^{+\cdot}$, $MV^{+\cdot} \rightarrow MV^0$ and $DMV^{+\cdot} \rightarrow DMV^0$ (a–d, respectively). Compound **2** (dotted line in Figure 9) showed two reversible one-electron reduction peaks (a′ and c′) and one reversible two-electron reduction peak (b′). We assigned the one-electron reduction peaks to $MV^{2+} \rightarrow MV^{+\cdot}$ and $DMV^{+\cdot} \rightarrow DMV^0$, respectively. The reversible two-electron reduction peak was due to the overlap of the $MV^{+\cdot} \rightarrow MV^0$ and $DMV^{2+} \rightarrow DMV^{+\cdot}$ reductions. We observed a clear indication of a strong electrostatic interaction between the two guest moieties, as the observed potentials for the reduction of **1** and **2** were different from those observed for free MV^{2+} and DMV^{2+} (Table 1).

In water, the CV charts of **1** and **2** (see the Supporting Information) did not show good reversibility, and the reduction processes were difficult to determine due to the hydrophobic nature of the multiply reduced compounds. Therefore, we performed Differential Pulse Voltammetry (DPV) measurements, which gave a good indication of the primary reduction potentials of **1** and **2** (Figure 10).

For **2**, we observed only two peaks with a current intensity ratio of 1:3. We assigned the one-electron reduction peak (a′) at –0.504 V vs. SCE to $MV^{2+} \rightarrow MV^{+\cdot}$. The three-electron reduction peak (b′) at –0.806 V vs. SCE indicated the second electron reduction of MV^{2+} ($MV^{+\cdot} \rightarrow MV^0$), which coincides with the $DMV^{2+} \rightarrow DMV^0$ double reduction. In the case of **1**, where there is a stronger interac-

tion between the two viologens, we observed three peaks instead, with a current intensity ratio of 1:1:2. We assigned the first one-electron reduction peak (a) at –0.438 V vs. SCE to the $MV^{2+} \rightarrow MV^{+\cdot}$ reduction and the second reduction peak (b) at –0.685 V vs. SCE to the first reduction of DMV^{2+}, $DMV^{2+} \rightarrow DMV^{+\cdot}$. We assigned the two-electron reduction peak (c) at –0.851 V vs. SCE to the second reduction of both attached viologens. We based the assignment on previously reported data from a similar system composed of a ruthenium complex.[34] The electrochemical data in water confirmed that the length of the linkers in **1** and **2** clearly affects the reduction potential of the two viologen units, most likely through electrostatic interactions, and that the $MV^{2+} \rightarrow MV^{+\cdot}$ reduction takes place first, well separated from other reduction processes.

To understand the interaction of CB[8] with **1** and **2**, we performed electrochemistry studies with the host (Figure 11). With 0.5 equiv. of CB[8], the redox potentials corresponding to the $MV^{2+} \rightarrow MV^{+\cdot}$ reduction in **1** and **2** decreased by 0.045 and 0.054 V, respectively. We performed the same measurements on free DMV^{2+} and MV^{2+} in solution with 0.5 equiv. of CB[8] (see the Supporting Information) and also observed small potential shifts. Since we had already established that, in both cases, the host was mainly positioned on the DMV^{2+} moiety, the decrease of the reduction potential of the MV moiety in **1** and **2** suggested the CB[8] had moved from DMV^{2+} to $MV^{+\cdot}$ during the electrochemical reduction process.

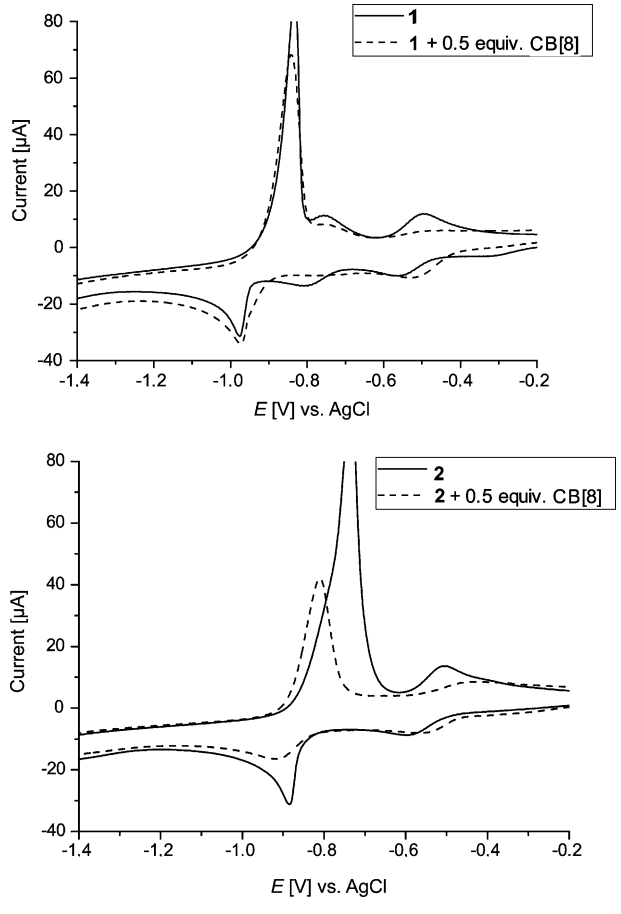

Figure 11. CVs of compound **1** (above) and **2** (below) in the presence (dashed line) or absence (solid line) of 0.5 equiv. of CB[8] at 1 mM in a pH 7 phosphate buffer with 0.1 M NaCl. The reference electrode was Ag/AgCl in pH 7 buffer, measured at a scan rate of 0.1 V s^{-1}, and the working electrode was a glassy carbon disk (3 mm diameter). The first reduction peak in both figures corresponds to $MV^{2+}/MV^{+\cdot}$.

Spectroelectrochemistry

To further study the first reduction of MV^{2+}, we performed spectroelectrochemical measurements on an aqueous solution of **1**. After degassing the solution with nitrogen, we introduced electrons at a potential of –0.56 V vs. SCE. In the absence of CB[8], only $MV^{+\cdot}$ formed in **1**, as indicated by the blue colour of the solution and the characteristic peaks at 397 and 600 nm in the UV/Vis spectrum (see Figure 12). However, upon the addition of 0.5 equiv. of CB[8] and a reduction at the same potential (–0.56 V vs. SCE), the peaks at 397 nm and 600 nm disappeared. Instead, the solution became purple, and we observed very strong peaks at 370, 550 and 880 nm in the UV/Vis spectrum, attributed to the formation of $MV^{+\cdot}$ dimers inside the

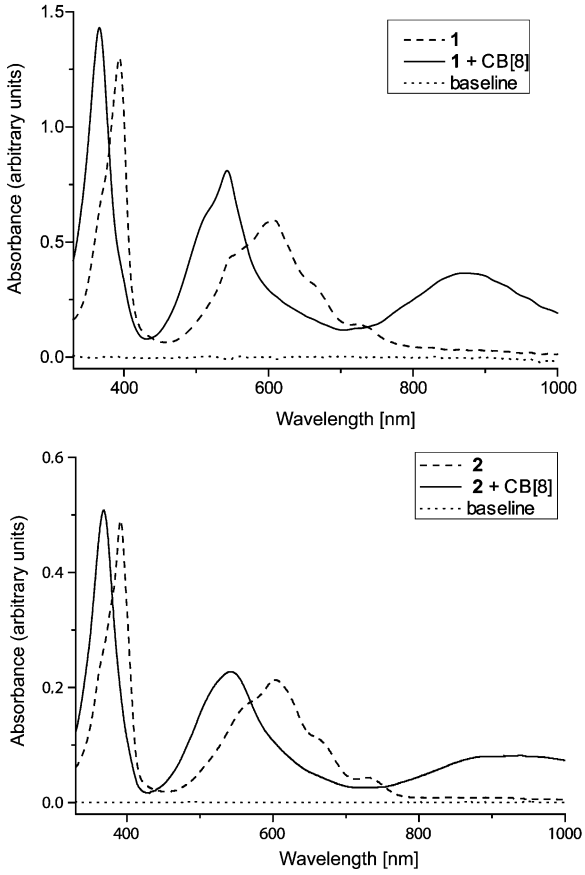

Figure 12. UV/Vis spectroelectrochemistry of **1** (top panel) and **2** (bottom panel) in water. The potential was applied at –0.56 and –0.66 V vs. SCE, respectively. Compound only is indicated by a dashed line, compound + 0.5 equiv. of CB[8] is indicated by a solid line and the dotted line was recorded before potential was applied (baseline).

CB[8] cavity (Figure 12, top panel).[12] We observed similar phenomena with **2** (Figure 12, bottom panel). Upon the removal of the potential and exposure of the cuvette to air, the solution became colourless, and the absorption bands between 300 and 1000 nm disappeared. We repeated this process several times.

Since only $MV^{+\cdot}$ could be generated at the applied potential, and the $MV^{+\cdot}$ dimer did not form in the absence of CB[8], we interpret our above result to indicate that the CB[8] host had moved from a position on DMV^{2+} to a position on $MV^{+\cdot}$ in **1** with the simultaneous formation of a stable $MV^{+\cdot}$ dimer inside the CB[8] cavity. The stabilising effect of $MV^{+\cdot}$ seen with the electrochemical measurements agrees with this interpretation. The reason why the stabilising effect observed for the **1**-CB[8] complex was smaller than that observed for the MV^{2+}-CB[8] complex is probably the need for the movement of the host. The addition of molecular oxygen can then move the CB[8] back to the position on the DMV^{2+}, due to the quenching of $MV^{+\cdot}$, as evidenced by ^1H NMR measurements. The electrochemically induced movement of CB[8] between the two viologen units is illustrated in Scheme 4. The same processes can also occur with **2**, indicating that the linkers (either 3 or 6 carbons in length) have no influence on the movement of CB[8] (Figure 12, bottom panel).

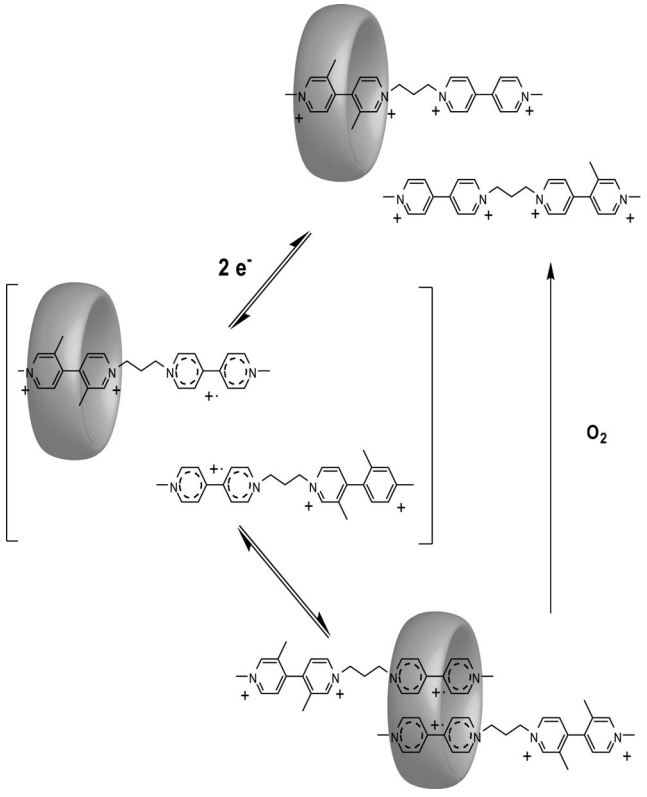

Scheme 4. Electrochemically induced movement of CB[8] from one position to another on **1**.

Conclusions

We studied the interactions of CB[8] and DMV^{2+} by ^1H NMR, ESI-MS and electrochemistry. We demonstrated that CB[8] selectively binds to DMV^{2+} in a mixture of DMV^{2+} and MV^{2+} or when the two viologens are covalently linked to each other by carbon chains of different length as in **1** and **2**. By the selective electrochemical reduction of MV^{2+} in **1** or **2**, the CB[8] unit was forced to move from the DMV unit to the MV unit. This movement was driven by the formation of the $MV^{+\cdot}$ dimer inside the CB[8] cavity. Upon the quenching of $MV^{+\cdot}$ by oxygen, CB[8] moved back to the DMV unit in both **1** and **2**. These reversible processes, driven by electrochemistry and oxygen, might be very useful for the design of more advanced supramolecular devices. Studies of systems consisting of **1** and **2** covalently linked to a photo-active $Ru(bpy)_3$ and interactions with CBs triggered by external light are in progress.

Experimental Section

General: ^1H and ^{13}C NMR spectra were obtained with a Bruker AVANCE 500 MHz instrument, and chemical shifts are reported relative to the residual signal (δ = 4.79 ppm) from D_2O. High-resolution mass spectrometry (HRMS) was performed with a Q-Tof mass spectrometer (Micromass, Manchester, England). ESI-MS was recorded with a Finnegan LCQ advantage spectrometer.

Electrochemistry: Cyclic voltammetry was carried out with a three-compartment cell connected to an Autolab potentiostat with a General Purpose Electrochemical System (GPES) electrochemical interface (Eco Chemie, B.V., Utrecht, The Netherlands). The working electrode was a freshly polished, glassy carbon disk (3 mm diameter), and the counter electrode was a platinum wire. Potentials were measured vs. a nonaqueous Ag/Ag^+ reference electrode (CH instruments, 10 mM $AgNO_3$ in acetonitrile) and converted to SCE by adding 300 mV to the measured value. Solutions were prepared from dry acetonitrile containing about 1 mM of the analyte and 0.1 M tetrabutylammonium hexafluorophosphate (Fluka, electrochemical grade, dried at 373 K for 48 h) as the supporting electrolyte. Before each measurement, oxygen was removed by bubbling argon through the solution for 20 min; the samples were kept under argon during measurement. In water, Cl^- was the counterion used, the reference electrode was Ag/AgCl in KCl, and the supporting electrolyte was a pH 7 phosphate buffer; measurements were converted to SCE by subtracting 45 mV from the measured value.

Spectroelectrochemistry: The measurements were performed using a spectroelectrochemical cell from CH instruments. The electrolysis to reduce the compounds was achieved by applying a potential at the Pt-net working electrode with an electrochemical workstation from CH instruments. The light source was a DH-2000 BAL, UV/Vis/NIR light source from MicroPack, connected to a personal computer.

Materials: 3-Methyl-4-(3-methylpyridin-4-yl)pyridine, DMV^{2+}, DMV^+ and MV^+ were synthesized according to literature procedures.[41–42] To make the DMV^{2+} soluble in water, chloride ions were introduced by anion exchange as described below. CB[8] and other materials employed were commercially available and used as supplied without purification. Solvents were dried by standard procedures.

Compounds **1** and **2** were prepared using a modified literature procedure.[40] A solution of dibromoalkane (16.8 mmol) and **I** (1.68 mmol) in CH_3CN (100 mL) was refluxed for 36 h. After the solution was cooled to room temp., the solution was filtered to yield a red precipitate **II**. The counter anion was exchanged with

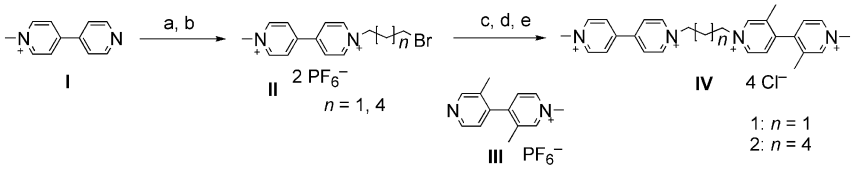

Scheme 5. a) Dibromoalkane, MeCN, reflux; b) NH_4PF_6, H_2O, room temp.; c) MeCN, reflux; d) NH_4PF_6, H_2O, room temp.; e) Et_4NCl, acetone, room temp.

NH_4PF_6 to provide **II**·PF_6. A solution of **II**·PF_6 (1.5 mmol) and **III**·PF_6 (4 mmol) in CH_3CN (15 mL) was refluxed for 6 d under nitrogen (Scheme 5). After the mixture was cooled to room temp., the solvent was removed under reduced pressure. The crude product was purified by column chromatography on silica gel with MeCN/H_2O/saturated KNO_3 (20:1:1 → 10:1:1 → 2:1:1) as the eluent. Pure **IV** was collected, and the counter anion was changed from NO_3^- to Cl^- by anion exchange, as described below.

Compound 1: Yield 56%. ^{1}H NMR (500 MHz, D_2O): δ = 9.24 (d, J = 6.7 Hz, 2 H), 9.10 (s, 1 H), 9.08 (d, J = 6.8 Hz, 2 H), 9.00 (d, J = 6.3 Hz, 1 H), 8.95 (s, 1 H), 8.85 (d, J = 6.3 Hz, 1 H), 8.63 (d, J = 6.7 Hz, 2 H), 8.55 (d, J = 6.7 Hz, 2 H), 8.07 (d, J = 6.2 Hz, 1 H), 7.97 (d, J = 6.2 Hz, 1 H), 5.00 (t, J = 8 Hz, 2 H), 4.94 (t, J = 8 Hz, 2 H), 2.94 (m, 2 H), 2.32 (s, 3 H), 2.30 (s, 3 H) ppm. ^{13}C NMR (125 MHz, D_2O): δ = 152.36, 151.07, 150.80, 149.60, 146.57, 146.36, 145.86, 145.71, 143.06, 142.43, 138.19, 137.22, 127.37, 127.36, 126.95, 126.70, 58.23, 58.17, 48.36, 48.26, 31.82, 16.32, 16.25 ppm. HRMS: calcd. for [1^+ – $1Cl^-$]$^+$ 517.1693; found 517.1665.

Compound 2: Yield 47.5%. ^{1}H NMR (500 MHz, D_2O): δ = 9.15 (d, J = 6.6 Hz, 2 H), 9.07 (d, J = 6.5 Hz, 2 H), 9.01 (s, 1 H), 8.95 (s, 1 H), 8.91 (d, J = 6.2 Hz, 1 H), 8.84 (d, J = 6.1 Hz, 1 H), 8.57 (d, J = 6.4 Hz, 2 H), 8.55 (d, J = 6.5 Hz, 2 H), 8.01 (d, J = 6.1 Hz, 1 H), 7.98 (d, J = 6.2 Hz, 1 H), 4.77 (m, 2 H), 4.70 (m, 2 H), 4.53 (s, 3 H), 4.48 (s, 3 H), 2.31 (s, 6 H), 2.14 (m, 4 H), 1.53 (m, 4 H) ppm. ^{13}C NMR (125 MHz, D_2O): δ = 150.09, 149.81, 146.52, 146.30, 145.58, 145.33, 143.02, 142.18, 137.69, 137.27, 127.34, 127.03, 126.68, 61.98, 61.86, 48.37, 48.19, 30.40, 30.38, 24.90, 24.89, 16.34, 16.26 ppm. HRMS: calcd. for [2^+ – $4Cl^-$]$^{4+}$ 113.5774; found 113.5779.

Anion Exchange. (a) From Bromide/Iodide to Hexafluorophosphate: The viologen bromide/iodide was dissolved in water. Upon the addition of aqueous NH_4PF_6, the hexafluorophosphate salt precipitated. The precipitate was collected by filtration and washed with H_2O to provide the desired compound.

(b) From Hexafluorophosphate to Chloride: The compound was dissolved in acetone. Upon the addition of Bu_4NCl in acetone, the chloride salt precipitated. The precipitate was collected by filtration and washed with acetone to provide the desired compound.

Supporting Information (see also the footnote on the first page of this article): ^{1}H-NMR, HRMS, CV, and UV/Vis spectral data (17 pages).

Acknowledgments

We acknowledge the Swedish Research Council, Swedish Energy Agency and the K & A Wallenberg foundation for financial support of this work.

[1] K. Kim, *Chem. Soc. Rev.* **2002**, *31*, 96–107.
[2] J. W. Lee, S. Samal, N. Selvapalam, H.-J. Kim, K. Kim, *Acc. Chem. Res.* **2003**, *36*, 621–630.
[3] K. Kim, N. Selvapalam, D. H. Oh, *J. Incl. Phenomena Macrocycl. Chem.* **2004**, *50*, 31–36.
[4] S. Liu, C. Ruspic, P. Mukhopadhyay, S. Chakrabarti, P. Y. Zavalij, L. Isaacs, *J. Am. Chem. Soc.* **2005**, *127*, 15959–15967.
[5] H. Tian, Q. C. Wang, *Chem. Soc. Rev.* **2006**, *35*, 361–374.
[6] K. Kim, N. Selvapalam, Y. H. Ko, K. M. Park, D. Kim, J. Kim, *Chem. Soc. Rev.* **2007**, *36*, 267–279.
[7] Y. H. Ko, E. Kim, I. Hwang, K. Kim, *Chem. Commun.* **2007**, 1305–1315.
[8] J. Lagona, P. Mukhopadhyay, S. Chakrabarti, L. Isaacs, *Angew. Chem. Int. Ed.* **2005**, *44*, 4844–4870.
[9] H.-J. Kim, J. Heo, W. S. Jeon, E. Lee, J. Kim, S. Sakamoto, K. Yamaguchi, K. Kim, *Angew. Chem. Int. Ed.* **2001**, *40*, 1526–1529.
[10] W. Ong, M. Gómez-Kaifer, A. E. Kaifer, *Org. Lett.* **2002**, *4*, 1791–1794.
[11] H.-J. Kim, W. S. Jeon, Y. H. Ko, K. Kim, *Proc. Natl. Acad. Sci. USA* **2002**, *99*, 5007–5011.
[12] W. S. Jeon, H.-J. Kim, C. Lee, K. Kim, *Chem. Commun.* **2002**, 1828–1829.
[13] W. S. Jeon, A. Y. Ziganshina, J. W. Lee, Y. H. Ko, J.-K. Kang, C. Lee, K. Kim, *Angew. Chem. Int. Ed.* **2003**, *42*, 4097–4100.
[14] W. Ong, A. E. Kaifer, *Angew. Chem. Int. Ed.* **2003**, *42*, 2164–2167.
[15] Y. H. Ko, K. Kim, J.-K. Kang, H. Chun, J. W. Lee, S. Sakamoto, K. Yamaguchi, J. C. Fettinger, K. Kim, *J. Am. Chem. Soc.* **2004**, *126*, 1932–1933.
[16] K. Kim, D. Kim, J. W. Lee, Y. H. Ko, K. Kim, *Chem. Commun.* **2004**, 848–849.
[17] W. Ong, A. E. Kaifer, *J. Org. Chem.* **2004**, *69*, 1383–1385.
[18] W. S. Jeon, E. Kim, Y. H. Ko, I. Hwang, J. W. Lee, S.-Y. Kim, H.-J. Kim, K. Kim, *Angew. Chem. Int. Ed.* **2005**, *44*, 87–91.
[19] I. Yildiz, M. Raymo, F. Tomasulo, *Proc. Natl. Acad. Sci. USA* **2006**, *103*, 11457–11460.
[20] V. Sindelar, S. Silvi, S. E. Parker, D. Sobransingh, A. E. Kaifer, *Adv. Funct. Mater.* **2007**, *17*, 694–701.
[21] L. Yuan, R. Wang, D. H. Macartney, *J. Org. Chem.* **2007**, *72*, 4539–4542.
[22] X. Ma, Q. Wang, D. Qu, Y. Xu, F. Ji, H. Tian, *Adv. Funct. Mater.* **2007**, *17*, 829–837.
[23] Y. Ling, J. T. Mague, E. A. Kaifer, *Chem. Eur. J.* **2007**, *13*, 7908–7914.
[24] P. R. Ashton, R. Ballardini, V. Balzani, A. Credi, K. R. Dress, E. Ishow, C. J. Kleverlaan, O. Kocian, J. A. Preece, N. Spencer, J. F. Stoddart, M. Venturi, S. Wenger, *Chem. Eur. J.* **2000**, *6*, 3558–3574.
[25] V. Balzani, M. Clemente-León, A. Credi, B. Ferrer, M. Venturi, A. H. Flood, J. F. Stoddart, *Proc. Natl. Acad. Sci. USA* **2006**, *103*, 1178–1183.
[26] S. G. Sun, R. Zhang, S. Andersson, J. X. Pan, B. Akermark, L. Sun, *Chem. Commun.* **2006**, 4195–4197.
[27] S. G. Sun, R. Zhang, S. Andersson, J. X. Pan, D. Zou, B. Akermark, L. Sun, *J. Phys. Chem. B* **2007**, *111*, 13357–13363.
[28] J. W. Lee, I. Hwang, W. S. Jeon, Y. H. Ko, S. Sakamoto, K. Yamaguchi, K. Kim, *Chem. Asian J.* **2008**, *3*, 1277–1283.
[29] V. Sindelar, S. Silvi, A. E. Kaifer, *Chem. Commun.* **2006**, 2185–2187.

[30] D. Tuncel, Ö. Özsar, H. B. Tiftik, B. Salih, *Chem. Commun.* **2007**, 1369–1371.
[31] Y. Liu, X.-Y. Li, H.-Y. Zhang, C.-J. Li, F. Ding, *J. Org. Chem.* **2007**, *72*, 3640–3645.
[32] T. Ooya, D. Inoue, H. S. Choi, Y. Kobayashi, S. Loethen, D. H. Thompson, Y. H. Ko, K. Kim, N. Yui, *Org. Lett.* **2006**, *8*, 3159–3162.
[33] S. Chakrabarti, P. Mukhopadhyay, S. Lin, L. Isaacs, *Org. Lett.* **2007**, *9*, 2349–3552.
[34] V. Schild, D. vanLoyen, H. Dürr, H. Bouas-Laurent, C. Turro, M. Wörner, M. R. Pokhrel, S. H. Bossmann, *J. Phys. Chem. A* **2002**, *106*, 9149–9158.
[35] V. Sindelar, M. A. Cejas, F. M. Raymo, A. E. Kaifer, *New J. Chem.* **2005**, *29*, 280–282.
[36] V. Sindelar, M. A. Cejas, F. M. Raymo, W. Chen, S. E. Parker, A. E. Kaifer, *Chem. Eur. J.* **2005**, *11*, 7054–7059.
[37] P. Chen, M. Curry, T. J. Meyer, *Inorg. Chem.* **1989**, *28*, 2271–2280.
[38] A. Loder, J. W. Launikonis, A. W.-H. Mau, W. H. F. Sasse, D. Summers, L. A. Wells, *Aust. J. Chem.* **1982**, *35*, 1341–1355.
[39] N. A. McAskill, *Aust. J. Chem.* **1984**, *37*, 1579–1592.
[40] The *K* value reported by Kim et al. corresponds to the equilibrium between the cation radical dimer and the host.
[41] J. Rebek, T. Costello, R. Wattley, *J. Am. Chem. Soc.* **1985**, *107*, 7487–7493.
[42] M. Seiler, H. Dürr, *Synthesis* **1994**, 83–86.

Received: October 15, 2008
Published Online: January 29, 2009

